Near-surface velocity characterization via RVSP and multicomponent seismic refraction experiments

Darryl G. Parry and Don C. Lawton

Abstract

A shallow 3-C RVSP survey was performed at a site in northwest Calgary. Traveltime inversion of the RVSP first arrivals has been augmented with a detailed 6-C refraction survey in order to define the velocity structure of the near-surface zone penetrated by the well. A velocity model consisting of 3 layers was derived with Vp = 310 m/s, Vs = 210 m/s in the first layer, Vp = 660 m/s, Vs = 330 m/s in the second layer, and Vp = 1790 m/s, Vs = 1110 m/s in the third layer.

Introduction

A shallow 3-C reverse vertical seismic profile (RVSP) experiment was undertaken during the University of Calgary field school in August of 1993. The survey was obtained using a 30 m deep drillhole with sources placed at spacings of every metre. The sources were 60 gm boosters and were fired sequentially from deepest to shallowest. A total of 32 3-C OYO receivers were employed in each of two orthogonal receiver lines laid out at surface, oriented roughly east/west and north/south. The near offset to the wellbore was 2 metres and the receiver interval used was 2 metres.

The first arrival data obtained during that survey have been examined previously in an effort to define the near-surface velocity structure (Parry and Lawton, 1993). However, the velocity image thus obtained (Figure 1) was incomplete with regard to shear wave velocities. The direct arriving shear waves recorded from sources below 14 metres are interpreted to have been produced by P to S conversion upon transmission through an interface at about that depth. Similarly, the shear wave velocity in the upper 3 metres could not be determined from the first arrival RVSP data. P-wave energy produced by sources in that zone swamped all incoming shear wave signal.

In an effort to more completely delimit the near-surface velocity structure (especially with regard to S-waves), a detailed 6-C refraction survey was undertaken in June of 1994. The source components were an accelerated weight drop (compressional wave source) and a swinging hammer striking a weighted beam (shear wave source). Arrivals from these sources were received on orthogonal 3-C OYO geophones using a 120 channel DAS 1 recording system.
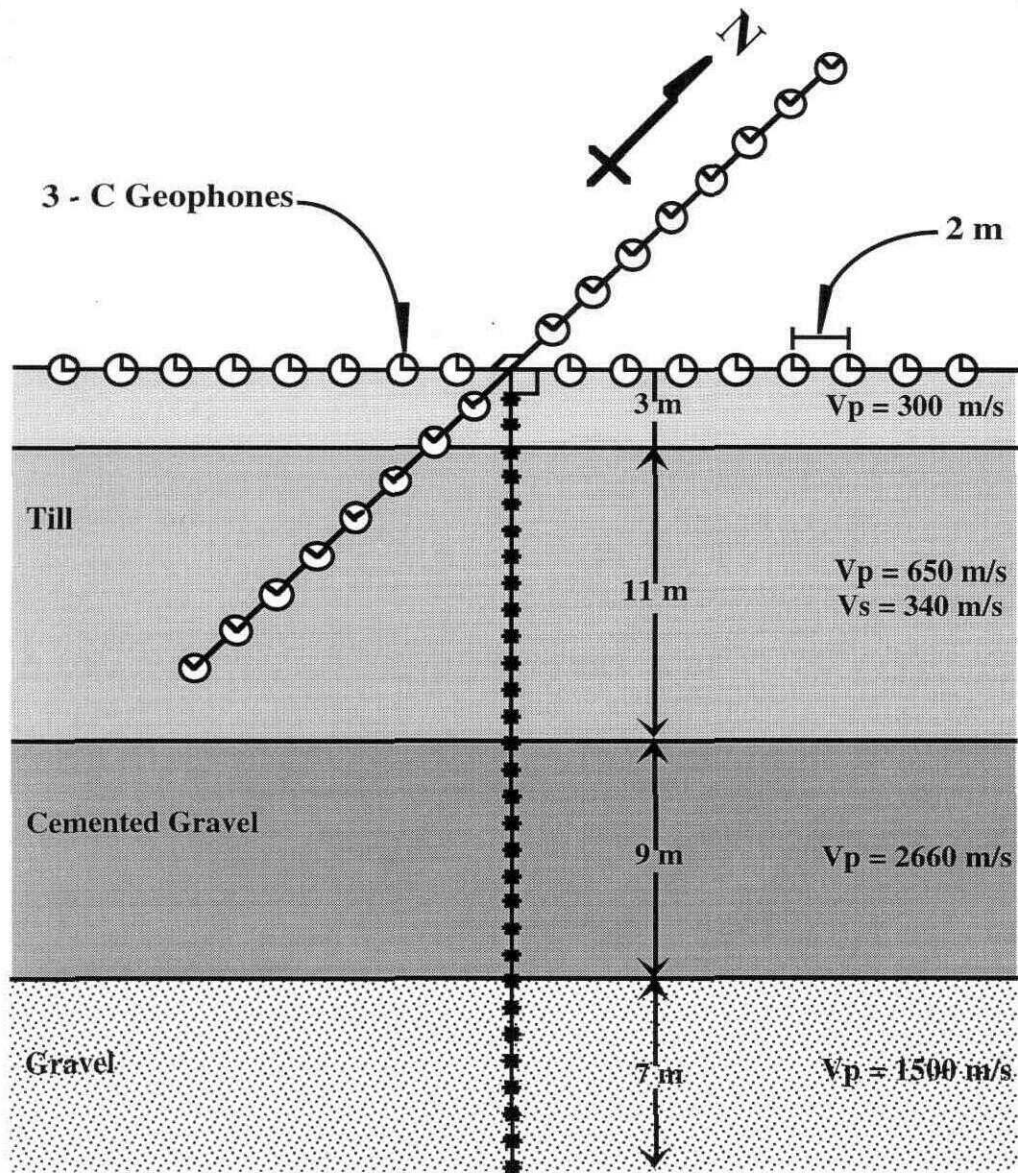
Fig. 1. RVSP Geometry and velocity structure from RVSP traveltime inversion. The stratigraphic interpretation is supported by geological study (Moran, 1987).

The velocity profile thus obtained provided a starting point for modelling the wavefield recorded by the RVSP survey. Such efforts lead to a better understanding of the ray geometry involved in the RVSP experiment and clarified the processing flow to be undertaken. This modelling was pursued by simplifying the stratigraphy investigated to flat plane features and iterating for reflection and refraction angles for a variety of source-receiver raypaths using this simplified geometry and Snell's law. This approach allows one to define the accuracy of the model based on the emergence location of a traced ray rather than by the number of ray angles (ie. fineness of the angular increment) used.

RVSP experiments can provide far more information than simple velocity structure. Reflections from impedance boundaries within the depth interval containing the sources and those from below that interval are recorded in such a survey. A

reflection profile obtained from an RVSP is readily matched to observed stratigraphy in a wellbore. It also shows improvement over conventional seismic profiling as the signal only travels through the shallow, highly attenuative earth once. The direct arriving wavefield, from which the velocity structure is derived, may be used to estimate the source signature for deconvolution purposes. It is also employed to separate the upgoing and downgoing wavefields in reflection processing.

VSP studies reference the wavefield to the receiver location. This makes sense as there is a simple distinction between the direct arriving (downgoing) and reflected (upgoing) wavefield at the receiver. That is not the case for RVSP, in which the wavefield is entirely upgoing at the receiver. Reference is therefore made to the shot for RVSP surveys. The direct arriving wavefield (and potentially some multiple energy) is upgoing and reflection energy (and potentially some multiple energy) is downgoing at the shot. Once this distinction is made, RVSP data can be processed in the same fashion as VSP data. RVSP common receiver gathers represent the same seismic events as would a VSP recorded with the shot located at the receiver location and geophones at the source locations. The raypaths travelled should be the same, but reversed (Chen et al., 1990).

Refraction Experiment

Survey Design and Field Program

Velocity information was the major objective of this experiment. Traveltime inversion of the RVSP direct arrival data provided an initial velocity picture, and this was used as the basis of refraction modelling for survey design. The receiver line was chosen to be 58.5 metres long, with 40 receivers (120 channels of 3-C receivers) laid out at an interval of 1.5 m. The line was oriented and centred along the east-west limb of the RVSP. P-wave sources were fired at 15 m intervals along the line, including offsets of 60.75 m from each end of the line. S-wave sources were employed at 30 m intervals starting 30.75 m west and ending 89.25 m east of the westmost receiver.

This geometry allowed recording at all receivers for every shot. The P-wave source used was a Bison Elastic Wave Generator (EWG). The word elastic in the name of this device refers not to its generating elastic waves, but to its mode of acceleration. A small motor is used to raise a weight against the resistance of several thick rubber (elastic) bands. This weight is then held in place and triggered on the demand of the operator. It provides clean, readily identifiable first breaks (Fig. 2) and has easily sufficient energy to produce clear first arrivals over the spread length used. Rayleigh waves are generated in abundance and dominate the later times on the shot record. One significant advantage to this device is the limited amount of environmental damage it produces. After a shot, the only obvious visual evidence left is an approximately 600 cm^2 area of flattened grass.

EWG Refraction Record
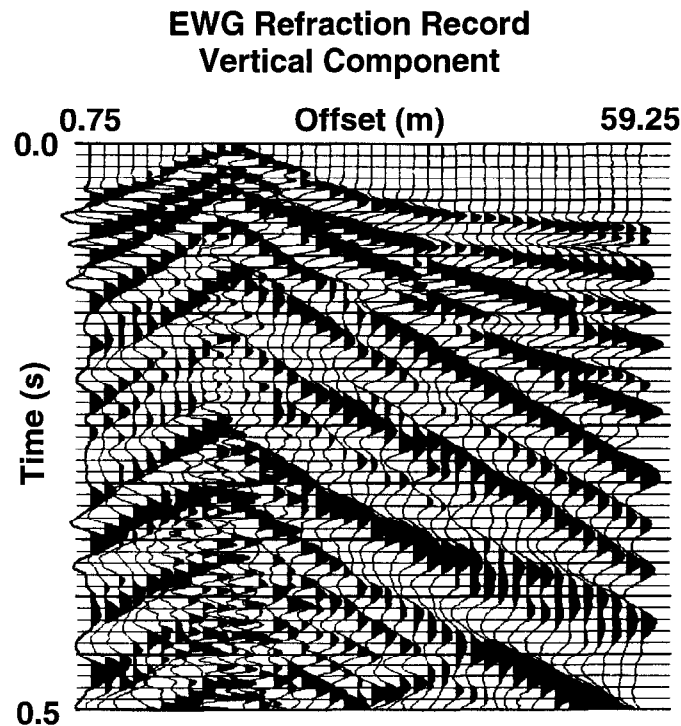**Vertical Component**

Fig. 2. Vertical component refraction record obtained using EWG device. Rayleigh waves dominate after the first breaks. The first arrivals are readily interpreted.

The S-wave source used in this experiment was a horizontal beam struck by a truck-mounted hammer (Lawton, 1990). The beam is coupled to the ground by angle iron attached to its base. A cable truck driven onto the beam for added mass has a pivoting assembly lashed to the cable cage. Pivots on both port and starboard sides of the truck allow generation of two opposite polarities of shear wave. Records thus obtained are differenced (port record minus starboard record) to remove the P-wave and enhance the shear wave arrivals. The procedure is quite robust and produces very readily interpretable shear wave records (Fig. 3). Ground roll is again dominant at late times, but the direct and refracted arrivals are unaffected.

Interpretation

The suite of refraction data acquired was interpreted using a variety of data reduction schemes. This survey was designed with a high degree of redundancy in order to phantom refraction arrivals across the spread so that a sophisticated interpretation could be carried out (Lankston, 1990). These reciprocal methods allow for higher lateral resolution in depth estimates from refraction profiling. Both the generalized reciprocal method (GRM) (Palmer, 1980), and the plus/minus method (Hagedoorn, 1959) were evaluated for use in this study. The result from the latter reduces to that of the former for an XY choice of 0.

While the GRM promises increased accuracy of depth estimations over the plus/minus method, it depends on a substantial degree of rugosity in the refractors under study. In order to make a proper choice of XY value (a critical parameter for GRM interpretation), one must visually estimate the goodness of fit of both the generalized time depth function and the velocity function (two intermediate steps in the GRM). The optimum XY value is chosen as that which provides the least deviation in the velocity function and the most in the generalized time depth function. This

deviation will be non-existent in the case of plane, flat-lying refractors. The refractors under study here are quite close to horizontal planar surfaces, so the interpretation scheme chosen was the plus/minus method.
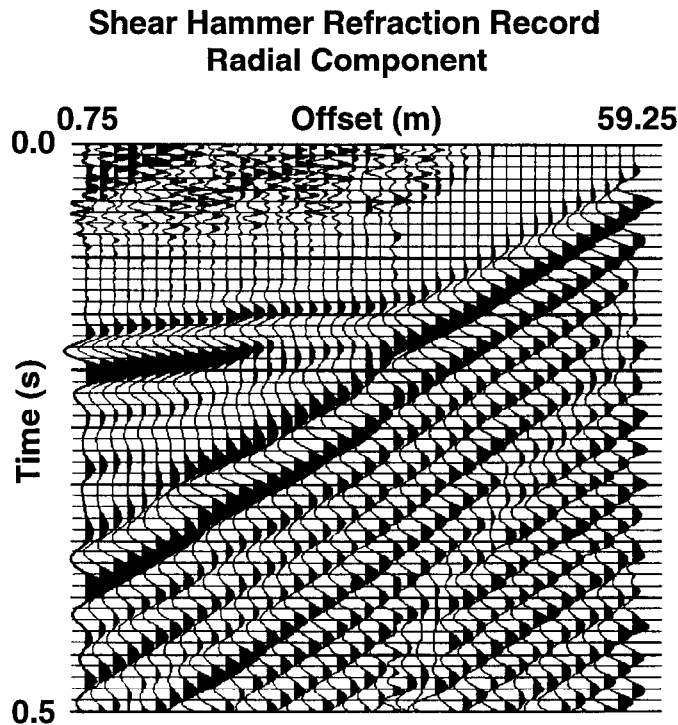
Shear Hammer Refraction Record
Radial Component

Fig. 3. Radial component refraction record. Shear hammer (S_h) source. This is a differenced record with P-wave energy reduced and S-waves enhanced.

Results

Figures 4 and 5 are traveltime curves for the compressional wave data and the shear wave data respectively. Phantoming these traveltimes from several shots along the profile provides the reciprocal traveltime curves shown in figures 6 and 7. A fully reciprocal suite of P-wave traveltimes is obtained for the uppermost two refractors while the S-wave source interval was such that phantoming could only provide a reciprocal suite for the second refracting interface. The depth estimates shown in Figure 8 are those for the P-wave survey, while those in Figure 9 are for the S-wave. The difference in depth estimates between the two is due to the application of the less robust slope/intercept method for first layer thickness determination in the S-wave data. The P-wave velocity estimate for the third layer is substantially lower for the refraction survey (1790 m/s) than for the RVSP (2660 m/s). This is attributed to a laterally discontinuous high-velocity cemented gravel immediately adjacent to the well. A three layer model is more reasonable for the survey site.
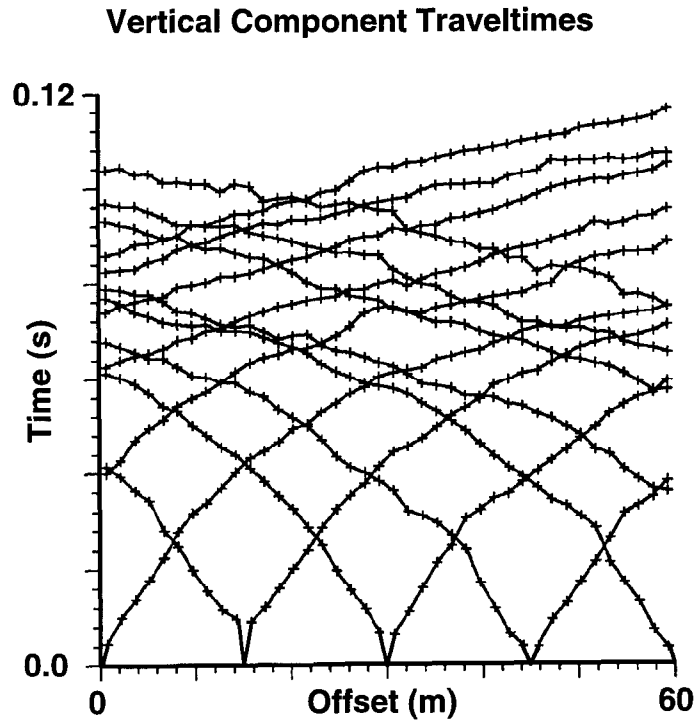
Vertical Component Traveltimes

Fig. 4. Raw traveltime curves for the vertical component refraction record.
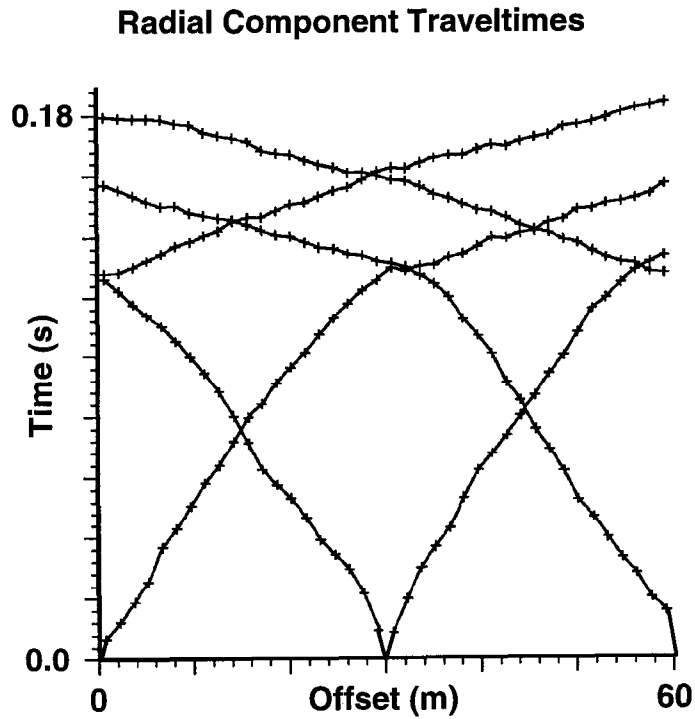
Radial Component Traveltimes

Fig. 5. Raw traveltime curves for the radial component refraction record.
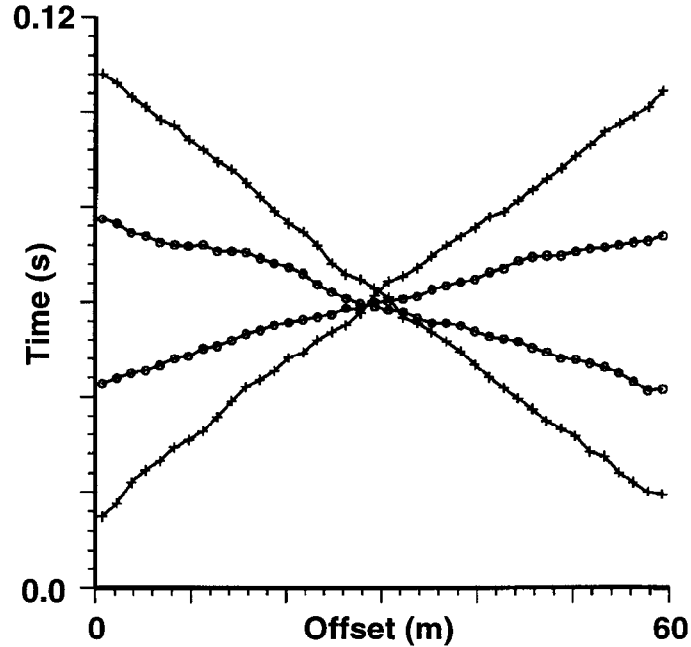
Vertical Component Reciprocal Traveltimes

Fig. 6. Reciprocal traveltime curves for vertical component refraction data. The time values presented here are phantomed from the raw traveltime data. The curves containing open circles are reciprocal traveltimes for the second refractor boundary. The curves containing crosses are for the first refractor.
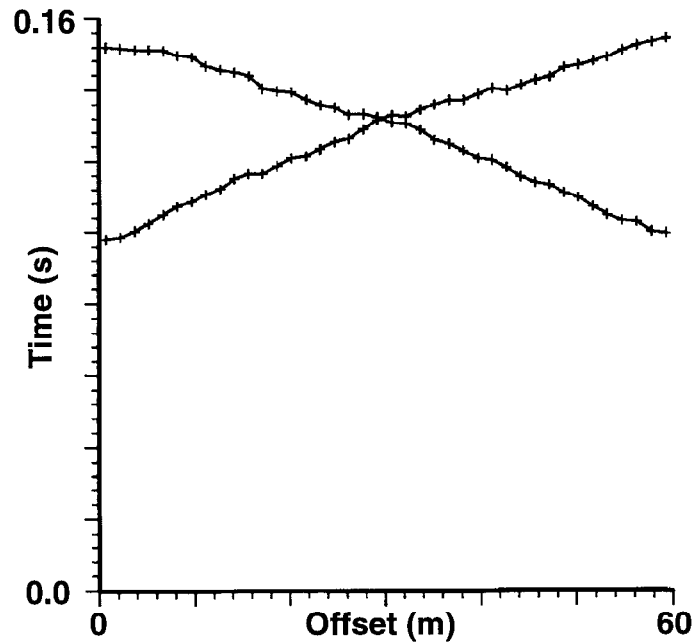
Radial Component Reciprocal Traveltimes

Fig. 7. Reciprocal traveltime curves for the second layer from radial component refraction data. A reciprocal curve could not be phantomed for the upper refractor.
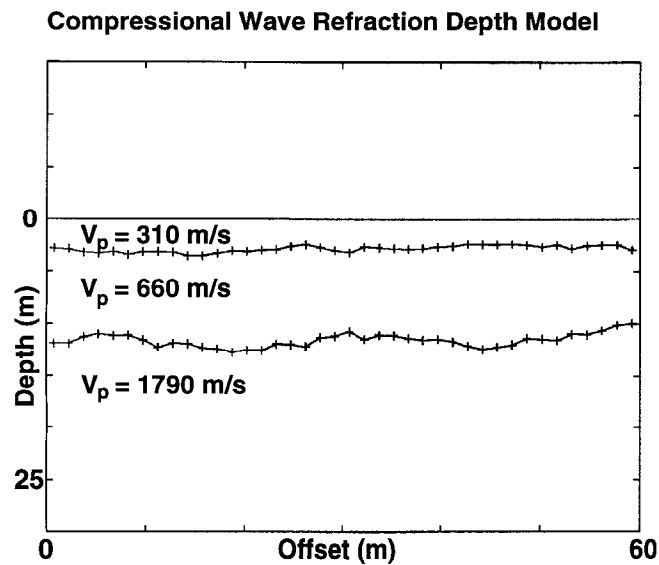
Compressional Wave Refraction Depth Model

Fig. 8. P-wave velocity structure from refraction survey.

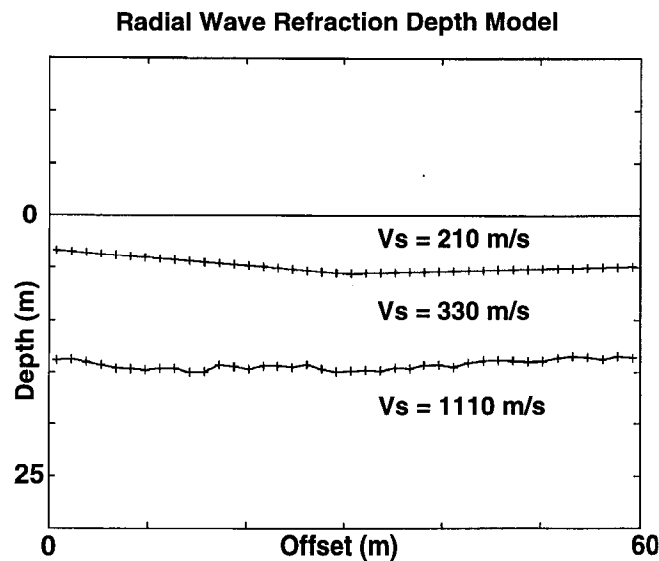**Radial Wave Refraction Depth Model**

Fig. 9. S-wave velocity structure from refraction survey. Upper layer is interpreted solely using the slope/intercept method.

RVSP Modelling

The geometry of the RVSP survey is such that many of the seismic events whose origin is within the wellbore depth interval follow raypaths with reflection angles greater than the critical angle. This suggests that the first arriving energy at varying offset (and especially at far offset) may not be direct arrival energy, but some more complicated path. This has implications for RVSP processing. In an effort to better understand the early arriving energy in the field data, the velocity structure obtained from refraction profiling and the RVSP geometry were used as a basis for traveltime modelling.

Nine possible events are considered (Figure 10). For sources in the uppermost velocity zone; direct arrivals, reflections, and refracted arrivals from both impedance boundaries are computed. In the second zone; direct arrivals, reflections and refractions from the layer 2/layer 3 boundary are computed. The lowermost zone only provides direct arrivals.
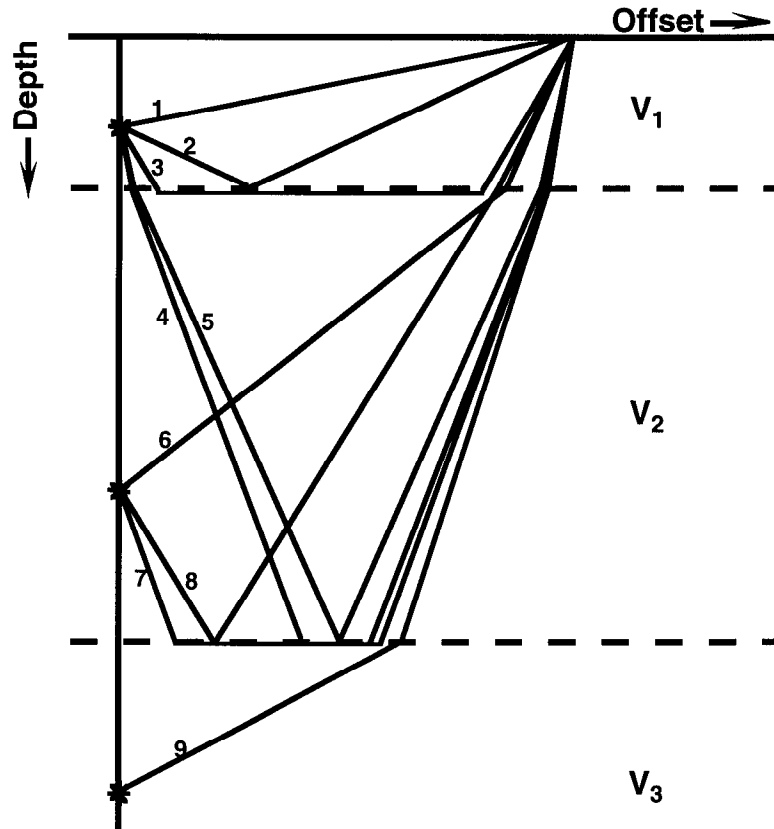
Modelled Raypaths

Fig. 10. Raypaths for seismic events considered in modelling. For sources in the first layer; 1) direct arrival, 2) ray reflected at first interface, 3) ray refracted at first interface, 4) ray refracted at second interface, 5) ray reflected at second interface. For sources in the second layer; 6) direct arrival, 7) ray refracted at second interface, 8) ray reflected at second interface. Sources in the third layer contribute 9) direct arrivals.

The program used to perform this modelling uses a series of equations depending only on geometry and Snell's law. These are readily derivable, but several of them require an iterative solution. This approach was chosen as it is more easily implemented than a ray-tracing scheme.

Results

Results are presented in common receiver form. Figure 11 shows modelled arrival time graphs for both P- and S-wave events for the offset extremes of 2 and 16 m. The near offset cases show no post-critical reflections for shear waves and refracted arrivals only from the layer 1/layer 2 boundary for the compressional wave source at 3 m depth. For the farthest offset receiver, post-critical reflections and refractions occur for all sources (P and S) originating in the uppermost two layers. Post-critical events

increase in number with increasing offset until all but direct arrivals are post-critical beyond 8 m for compressional waves and beyond 6 m for shear waves.
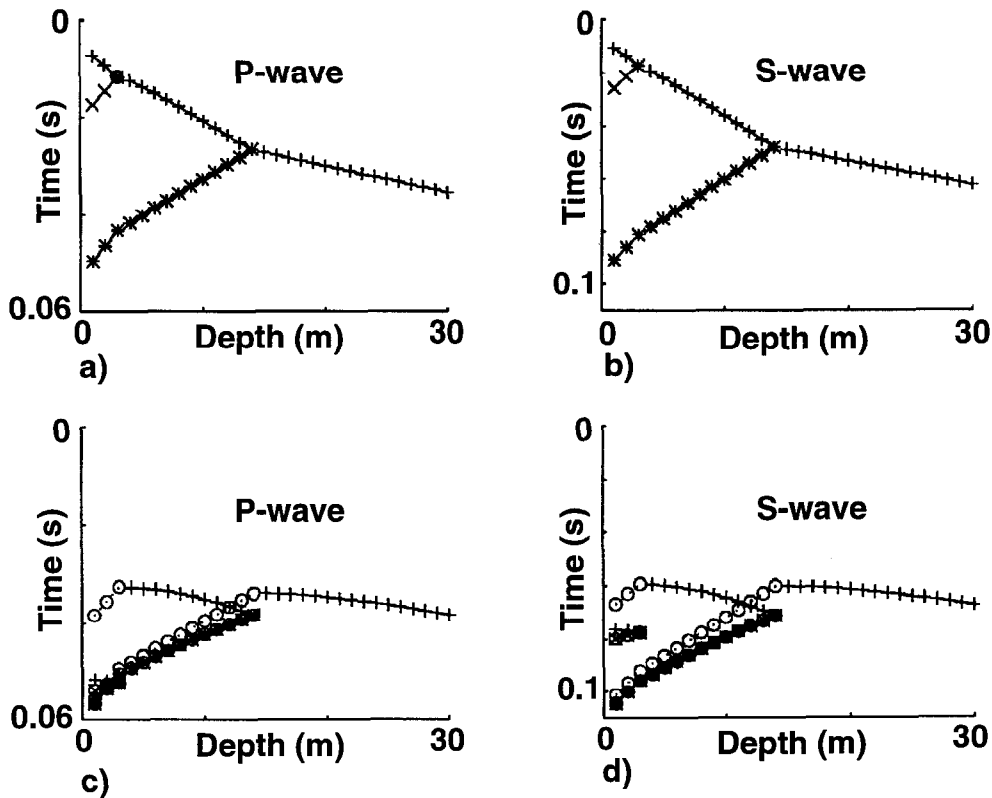
Traveltime Modelling

Fig. 11. RVSP traveltime models for the refraction velocity structure. Crosses indicate direct arrival travel paths (events 1, 6, and 9 in Fig. 10), x's are reflections from the first interface (event 2 in Fig. 10) , *'s are reflections from the second interface (events 5 and 8 in Fig. 10). Circles indicate travel paths including reflections past the critical angle. Open circles indicate head-wave arrivals (events 3, 4, and 7 in Fig. 10). a) is for a 2m offset P-wave receiver, b) is for a 2m offset S-wave receiver, c) is for a 16 m offset P-wave receiver, and d) is for a 16 m offset S-wave receiver. The first arriving energy follows a direct arrival path for all depths for the near offsets, but is alternatively direct arrival or head-wave arriving energy for the far offsets.

The modelling suggests that the near offset common receiver gathers can be treated as a normal VSP data suite with appropriate consideration given to the sense of direction of the seismic wavefields involved. The direct arrivals are not substantially obscured by other early arriving seismic energy (Figures 12 and 13). This approach has been applied to both the vertical and radial component common receiver gathers for 2 metres offset.
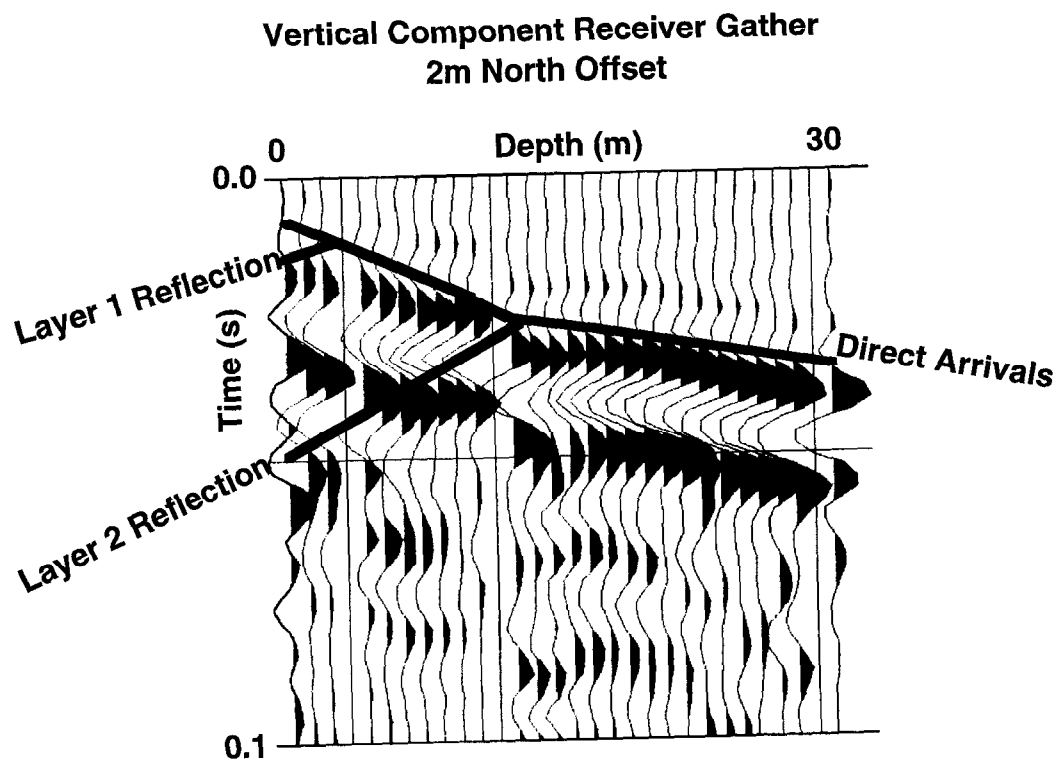
Vertical Component Receiver Gather
2m North Offset

Fig. 12. Modelled traveltimes overlain on early record section. Vertical component data for 2m north offset receiver.

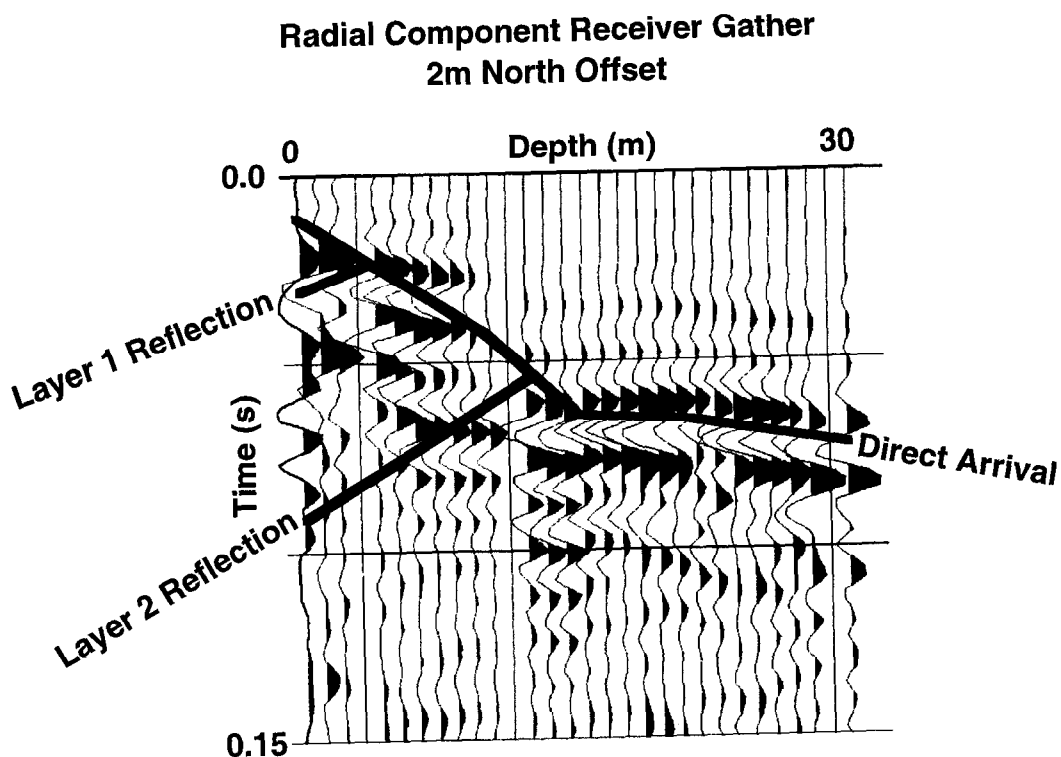**Radial Component Receiver Gather**
2m North Offset

Fig. 13. Modelled traveltimes overlain on early record section. Radial component data for 2m north offset receiver.

RVSP

Processing

The processing flow used for a near-offset RVSP is shown in Figure 14. Gathering, geometry and first break picking are essentially pre-processing steps. Gathering to common receiver domain provides the VSP approximation. First breaks and geometry are required for velocity determination and wavefield separation.

```
┌──────────────────────────────┐
│   Gather to Common Receiver   │
└──────────────────────────────┘
                │
        ┌───────────────┐
        │   Geometry    │
        └───────────────┘
                │
       ┌──────────────────┐
       │ Pick First Breaks │
       └──────────────────┘
                │
     ┌──────────────────────┐
     │ Wavefield Separation  │
     └──────────────────────┘
                │
    ┌────────────────────────┐
    │  Decon Design Upgoing   │
    └────────────────────────┘
                │
   ┌──────────────────────────┐
   │  Deconvolve Downgoing     │
   └──────────────────────────┘
                │
       ┌──────────────────┐
       │  Corridor Stack   │
       └──────────────────┘
```
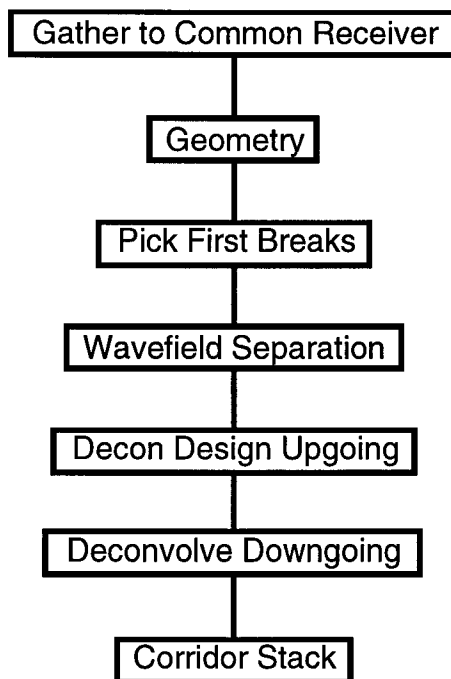
Fig. 14. Near-offset RVSP processing flow.

Wavefield separation is accomplished by filtering to remove events that are near to parallel to the first breaks. This is most commonly done by aligning the traces on first breaks, applying a median filter to the gather and subtracting the filtered output from the input gather (Kommedal and Tjostheim, 1989). Another technique is to transform the data to the f/k domain and effect wavefield separation there (Chen et al, 1990). The upgoing and downgoing waves should map into different areas in the f/k domain as they exhibit opposite dips in time.

The direct arrivals are used to design a deconvolution operator for the downgoing data set as they are assumed to well approximate the wavelet. The deconvolution operator is applied to the downgoing wavefield which is then bandpass filtered to improve S/N. Finally, the traces are muted to remove direct arrivals and late time arrivals which are dominated by noise and are stacked to produce the RVSP extracted trace (RET).

Figures 15 and 16 are gathers for the receiver 2 m west of the borehole (vertical and radial component respectively). The first arrivals of shear wave energy on the radial component are partially obscured by earlier arriving compressional waves. The

impulsive source used in this experiment suggests that the wavelet should be minimum phase, but the direct arrivals appear distinctly zero phase, probably resulting from instrument response.

Vertical Component Receiver Gather
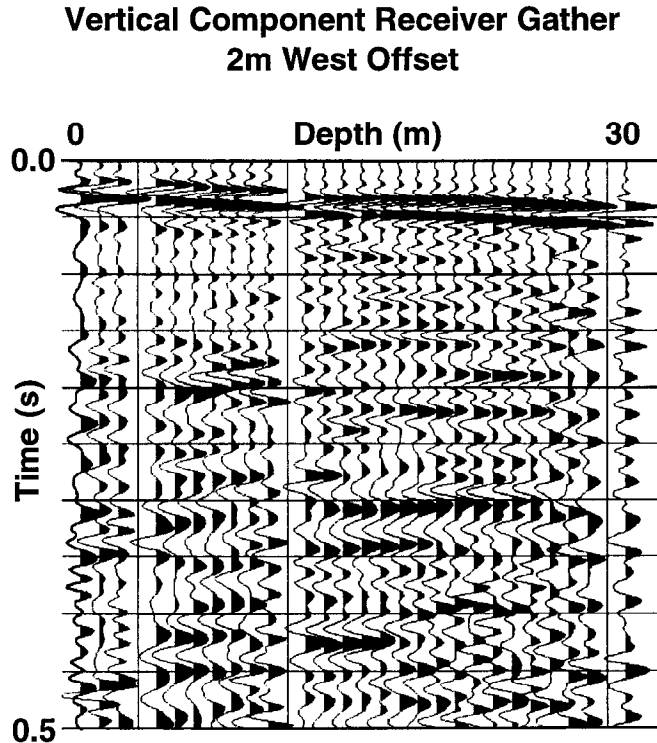**2m West Offset**

Fig. 15. Vertical component common receiver gather - 2m west offset receiver.

Several attempts at deconvolution were made for these data, none of which showed substantial improvement in data quality. Zero phase deconvolution was one of the attempted methods, suggested by the zero phase appearance of the direct arrivals. The final results reported here have not had any deconvolution applied to the data.

Wavefield separation was attempted via both f/k filtering and median filtering the aligned downgoing wavefield. In both cases the upgoing wavefield was severely affected in the process. Given the geometry used in this experiment, especially its extreme shallowness, the upgoing and the downgoing wavefields exhibit little difference in trace to trace moveout, so that any technique depending on velocity variation in the two wavefields will not effectively separate them. The decision was made to proceed with the stack without explicit wavefield separation. The upgoing wavefield should contribute less to the final gather as its stronger events are relatively early and partially muted. The stacking process should also reduce its effect.

Results

Final RET's and the aligned gathers from which they derive are shown in Figures 17 and 18. These were obtained from the 2 m west offset receiver. On the vertical data, a strong trough doublet manifests itself at 300-375 ms time, as does a strong peak at about 200 ms time. The trough/peak/trough triplet at about 130 to 150 ms is also evident on all near offset stacks. Correlatability for the other events in the zone 120-400 ms is less striking, possibly resulting from the brute stack approach to the RET generation.

The radial component data exhibit greater correlatability, perhaps because the slower travelling shear waves are more completely separated during processing. Events from about 220 ms to 480 ms on these stacks are all well correlated.
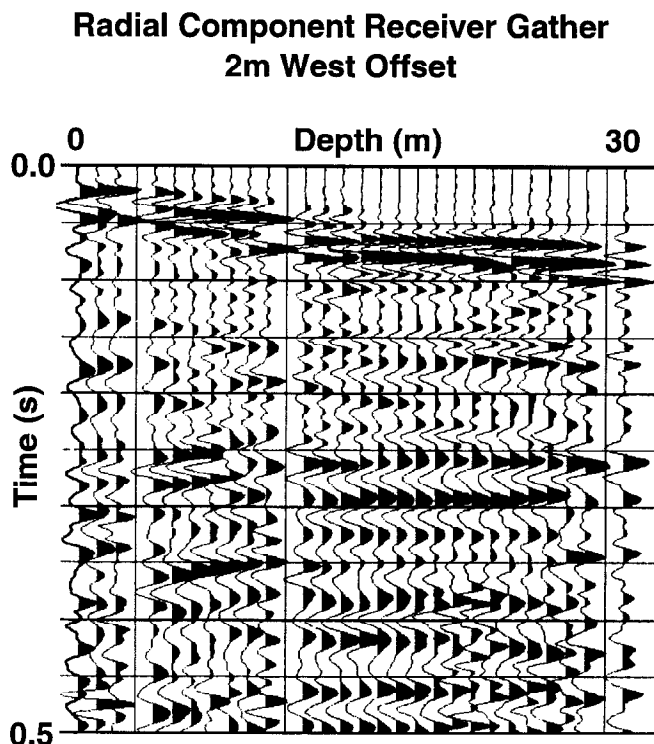
Radial Component Receiver Gather
2m West Offset

Fig. 16. Radial component common receiver gather - 2m west offset receiver.

Conclusions

Detailed 6-C refraction surveying provided increased confidence in the compressional wave velocity profile derived from RVSP traveltime inversion. It also provides more detail with regard to shear wave velocity structure. The upper 30 m of the earth at the survey site exhibit three distinct velocity zones; 0-3 m, 3-12 m, and 12-30+ m. Their corresponding velocity values are; Vp=330 m/s Vs = 210 m/s, Vp = 660 m/s Vs = 330 m/s, Vp = 1790 m/s Vs = 1110 m/s.

Traveltime modelling for the well interval arrivals suggests that a zero-offset VSP approach is suitable for processing the near offset receiver gathers from the RVSP survey. Post-critical reflections and headwave arrivals are observed at receivers offset more than 8 m in the P-wave case and 6 m in the S-wave case.

Very shallow RVSP surveys do not allow the full VSP processing approach to be implemented completely. Wavefield separation is particularly problematic as upgoing and downgoing waves differ little in trace to trace moveout. A brute stack approach with no wavefield separation beyond stacking shifted traces will still provide interpretable RETs.

Acknowledgements

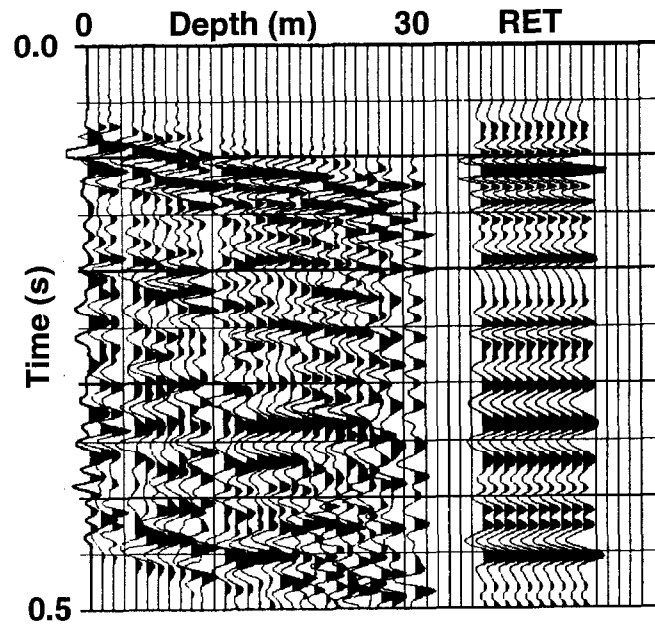**Vertical Component Receiver Gather and RET
2m North Offset**

Fig. 17. Aligned downgoing wavefield and RET. Vertical component data.

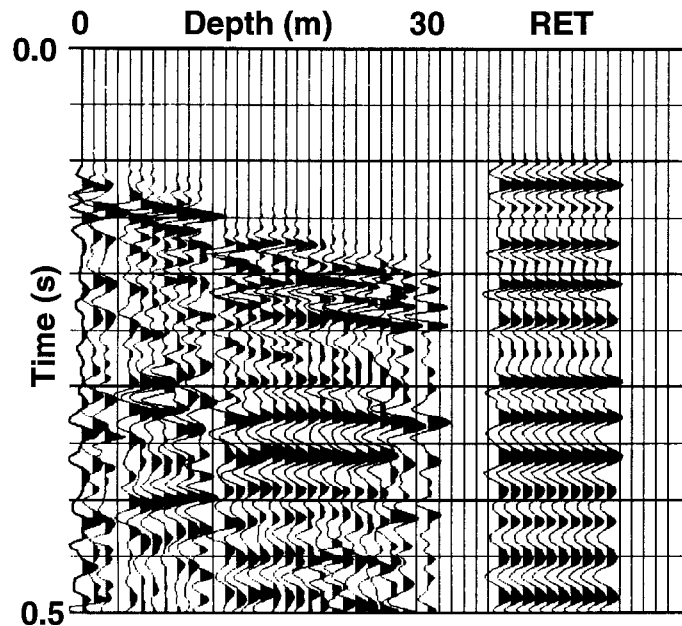**Radial Component Receiver Gather and RET**
2m North Offset

Fig. 18. Aligned downgoing wavefield and RET. Radial component data.

References

Chen, S.T., Zimmerman, L.J. and Tugnait, J.K., 1990, Subsurface imaging using reversed vertical seismic profiling and crosshole tomographic methods: Geophysics, 55(11), 1478-1487.

Hagedoorn, J.G., 1959, The plus-minus method for interpreting seismic refraction sections: Geophysical Prospecting, 7, 158-182.

Kommedal, J.H. and Tjostheim, B.A., 1989, A study of different methods of wavefield separation for application to VSP data: Geophysical Prospecting, 37, 117-142.

Lankston, R.W., 1990, High-resolution refraction seismic data acquisition and interpretation; in, Ward, S.H., Ed., Geotechnical and Environmental Geophysics: Volume I - Review and Tutorial: Society of Exploration Geophysicists.

Lawton, D.C., 1990, A 9-component refraction seismic experiment: Canadian Journal of Exploration Geophysics, 26(1&2), 7-16.

Moran, S.R., 1987, Surficial geology of the Calgary urban area: Alberta Research Council, Bulletin 53.

Palmer, D., 1980, The generalized reciprocal method of seismic refraction interpretation: Society of Exploration Geophysicists.

Parry, D.G., and Lawton, D.C., 1993, Analysis of direct wave arrivals in a shallow multi-offset reverse VSP: CREWES Project Research Report, Volume 5, 8.1-8.16.